

Optical and electrical properties of quantum composite of polyvinyl alcohol matrix with CdSe quantum dots

Zein K. Heiba^{1,3} · Mohamed Bakr Mohamed^{2,3} · N. G. Imam⁴ · Nasser Y. Mostafa^{1,5}

Received: 10 August 2015 / Revised: 10 October 2015 / Accepted: 11 October 2015 / Published online: 26 October 2015
© Springer-Verlag Berlin Heidelberg 2015

Abstract CdSe quantum dots (QDs) were prepared by a simple green route with CdSO₄ and Na₂SeSO₃ in aqueous solution. The as-prepared citrate-capped CdSe QDs were characterized by XRD and TEM. Single-phase cubic zinc blende structure was confirmed with uniform size and highly crystallized QDs of CdSe. Composite based on the decoration of polyvinyl alcohol (PVA) matrix with CdSe QDs was fabricated by the solution casting process. UV–vis absorption spectra confirmed the formation of composites with a refractive index which was enhanced with CdSe weight fraction wt%. Photoluminescence properties of CdSe@PVA composites at different CdSe QD weight fractions (wt%) were recorded. The emission colors were controlled by CdSe wt% and tuned with its particle size. The a.c. electrical conductivity was measured at temperatures from 300 to 493 K and at frequencies from 50 to 100 kHz. The dielectric constant was enhanced after inserting CdSe QDs into PVA matrix. The a.c. electrical conductivity results showed that PVA and CdSe@PVA composite films follow the overlap large polarons (OLP) model. Also,

the activation energy (E_a) decreased with the presence of CdSe in PVA polymer relative to pure PVA.

Keywords CdSe QDs · PVA · Composite · Optical · Dielectric

Introduction

Currently, production of low-cost, advanced, and environment-friendly “green” technology is the main aim of the scientific research work. Consequently, tailoring of novel, low-cost, and “green” nanohybrid composites from semiconductor quantum dots (QDs) and environment-friendly polymers is highly desired due to their potential applications in different fields of our life such as medical, optoelectronic, and technological ones [1]. Semiconductor QDs at polymer nanohybrid composites show promising and novel properties due to combination of unique chemical and optical characteristic features of semiconductor QDs and the own characteristic features of polymer networks (such as flexibility, high mechanical strength, and easy processability) [2].

Polyvinyl alcohol (PVA) is an environmentally friendly polymer; it is a biocompatible, nontoxic, noncarcinogenic, hydrophilic biodegradable organic material [3]. Also, PVA is a transparent optical material characterized by a high chemical resistance and a high ability of thin sheet (film) fabrication [4]. PVA has been broadly investigated for different medical, pharmaceutical, cosmetic, and agricultural applications [3]. Furthermore, PVA is a very good candidate as a polymeric host matrix in different potential nanohybrid composite-based polymer and quantum dot materials like CdSe [5]. Actually, due to its unique optical performance, involving photo stability, size-tunable band gap, optical absorption which is extended in the UV

✉ Mohamed Bakr Mohamed
mbm1977@yahoo.com

¹ Faculty of Science, Taif University, Taif, Kingdom of Saudi Arabia

² Physics Department, Taibah University, Tayba, Al-Madinah Al-Munawara, Saudi Arabia

³ Faculty of Science, Physics Department, Ain Shams University, Cairo, Egypt

⁴ Experimental Physics Department, Nuclear Research Center, Atomic Energy Authority, Cairo 13759, Egypt

⁵ Chemistry Department, Faculty of Science, Suez Canal University, Ismailia 41522, Egypt

region, and shining photoluminescence (PL), CdSe (QDs) is an optimum material for obtaining unique electronic and optical performance of quantum-confined semiconducting materials [6–8]. CdSe shows absorption edge at about 710 nm corresponding to a band gap value of 1.74 eV [1]. Accordingly, CdSe QDs have been broadly investigated for different applications, like cellular imaging, bio-probes, and solar cells [9]. As mentioned above, the integration between PVA polymeric matrix and CdSe QDs as a filler material to form a composite is expected to show promising performance in the highly advanced technology owing to the unique size-dependent photophysical, electrical, and chemical characteristics [1]. On the other hand and when CdSe QDs are loaded into PVA matrix, the size of CdSe particles are controlled because they are protected by thick surroundings. Since the fluorescence of CdSe QDs is a size-dependent property, at appropriate size, CdSe QDs show quantum confinement feature such that the QDs can show visible emission bands. These unique features make CdSe/PVA nanocomposite as a very good candidate for medical or

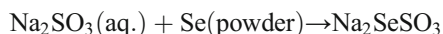
biological applications as a fluorescent biomarker with multicolor emission bands [2].

Therefore, herein, the present work aimed to prepare low-cost and environment-friendly nanohybrid composites that can be applied in biological or medical applications as a fluorescent biomarker.

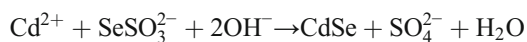
Experimental work

Synthesis of water-soluble CdSe QDs

Selenium powder (0.098 g) and Na_2SO_3 (0.5 g) were dissolved in Milli-Q water (20 mL); then they are mixed thoroughly in three-necked round-bottom flask and refluxed for 3.5 h using magnetic stirring. The black colure of Se disappeared and a clear solution was formed which suggested the complete conversion of Se into sodium selenosulfate (Na_2SeSO_3), according to the following equation:



The mixture was filtered through Whatman filter paper, after that the mixture was cooled down to ambient temperature. Then it was diluted to 25 mL in a standard measuring flask with Milli-Q water to prepare 50 mM Na_2SeSO_3 solution. This freshly prepared solution was used directly for CdSe QD synthesis. A classical synthetic procedure of the CdSe QDs is briefly described as follows: First, 7.2 mL of 0.2 M CdSO_4 solution and 0.3 g sodium citrate were added to 200 mL of double-distilled water with rapid stirring. The pH was adjusted to 8 units using 1 M NaOH solution. Then 6 mL of sodium selenosulfate solution (0.4 M) (containing about 2.4 mmol of Se precursor) was swiftly injected into the solution with rapid stirring. The $[\text{Cd}^{2+}]/[\text{Se}^{2-}]$ ratios were kept constant as 2.2 at room temperature for the growth of CdSe QDs according to the following equation:



At the end, methanol was added to precipitate CdSe QDs. The precipitated CdSe QDs were separated by centrifugation, further washed with methanol several times.

Preparation of CdSeQDs/PVA composite film

A clear solution of composite was obtained by dissolving 4 g of PVA powder in 100 mL of hot deionized water using a magnetic stirring. Then CdSe nanoparticles (0.1 and 0.5 %) were added to the solution and sonicated. The mixture was then poured into glass dishes and dried at 40 °C to get the films.

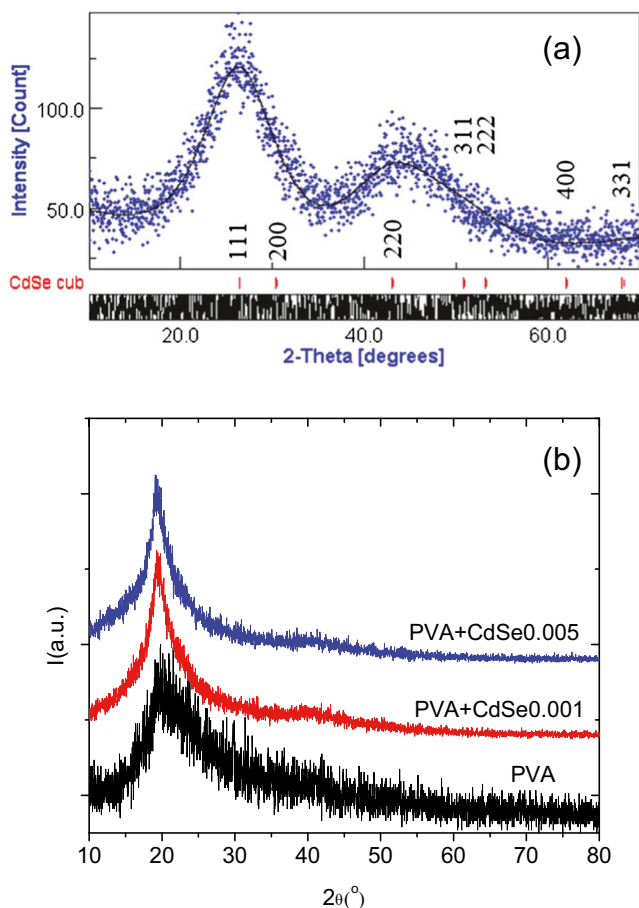


Fig. 1 **a** XRD pattern fitting resulting from Rietveld analysis of CdSe quantum dots. **b** XRD patterns for pure PVA and PVA loaded with different amounts of CdSe nanoparticles

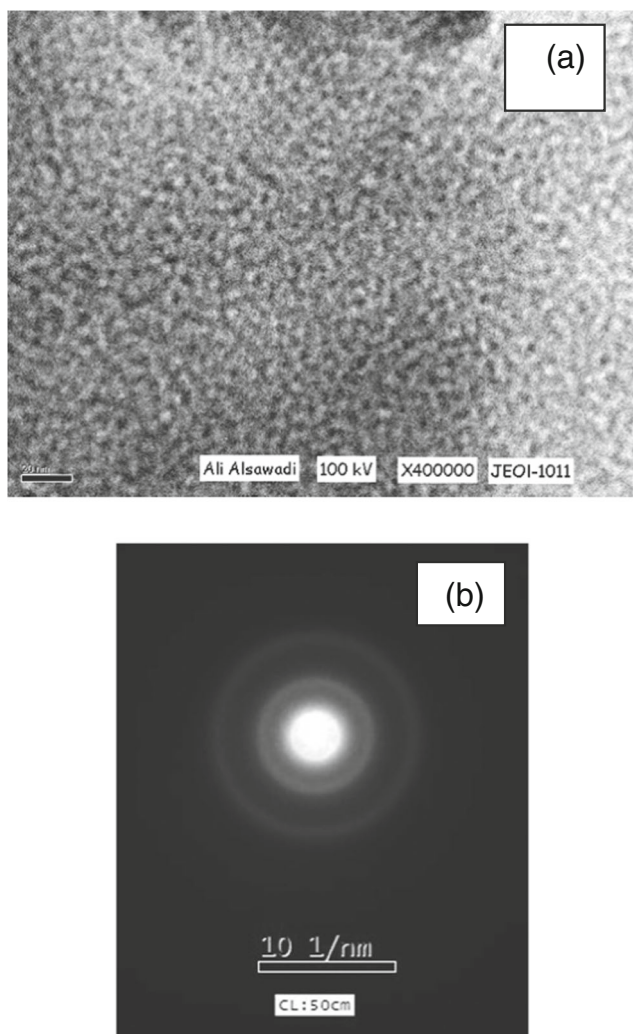


Fig. 2 **a** TEM image of CdSe QDs. **b** Selected area electron diffraction (SAED) of CdSe QDs

Measurements and instrumentations

X-ray powder diffraction (XRD) of the samples was performed by using PANalytical diffractometer (X'pert MPD) with Cu-K α source. The diffraction patterns were collected in 2θ range from 10 to 80°. To correct the instrumental broadening, LaB $_6$ standard was used. Rietveld profile analysis method [10] was used by applying MAUD software [11] in order to determine the crystal structure and microstructure of the refined samples. Transmission electron microscope (JTEM-1230, Japan, JEOL) was used to investigate the shape and particle size of the studied samples. UV spectra were measured by using UV-vis spectrophotometer (Model Tomos UV-1800) in the wavelength range from 1100 to 190 nm, in transmission mode. Photoluminescence (PL) measurements were collected by a luminescence spectrophotometer (RF-1501 SHIMADZU, Ltd.) with a

resolution of 1.0 nm at room temperature. The dielectric constant (ϵ') was calculated using the relation $\epsilon' = \frac{Cd}{\epsilon_0 A}$, where ϵ_0 is the permittivity of the free space, d is the thickness of the thin solid film in the form of disk with diameter of 1 cm and thickness of 3 mm, A is the area of its cross section (0.785 cm 2), and C is the measured value of the capacitance of the disk, using a complex impedance technique (LIA, SR510). In this work, the a.c. electrical measurements have been recorded at temperatures from 300 to 493 K and at frequencies from 50 to 100 kHz. By using the dielectric constant (ϵ') and dielectric loss tangent ($\tan\delta$), the dielectric loss factor ϵ'' of the samples can be calculated: $\epsilon'' = \epsilon' \tan\delta$. The a.c. conductivity of the sample was obtained from the following relation: $\sigma_{ac} = \epsilon' \epsilon_0 \omega \tan\delta$, where ω is the angular frequency.

Results and discussion

X-ray diffraction and morphological analysis

Figure 1a shows the XRD pattern fitting obtained from Rietveld analysis for the prepared CdSe QDs. For QDs

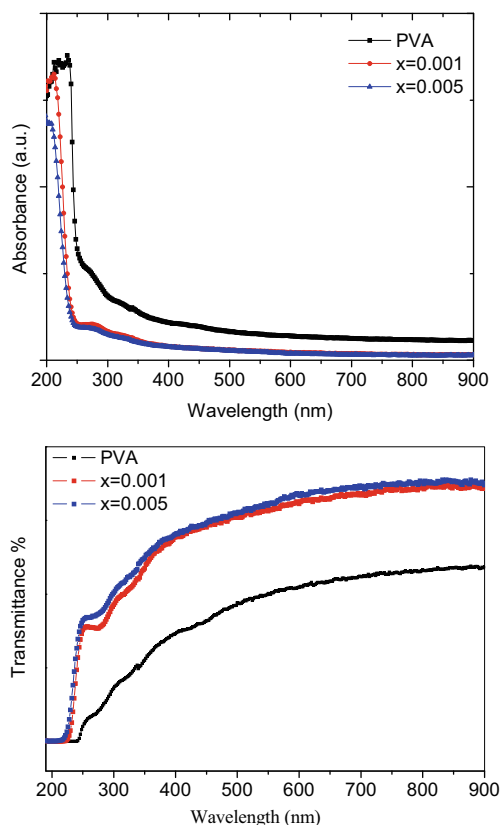


Fig. 3 Absorption and transmittance spectra of PVA and CdSe@PVA composites

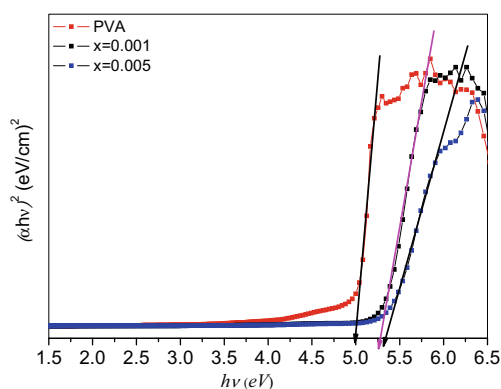


Fig. 4 Plot of $(\alpha h\nu)^2$ vs. $h\nu$ for pure PVA as well as for PVA and CdSe@PVA composites

chalcogenides, broad diffraction peaks are obtained with overlapping and structural phase analysis becomes confusing [12, 13]. Therefore, two structures were tried, hexagonal wurtzite and cubic zinc blende, but analysis showed that the present CdSe adapts cubic zinc blende structure with a lattice parameter of 6.057 Å and a mean grain size of 2 nm. Figure 1b depicts the XRD patterns obtained for pure PVA and PVA loaded with different amounts of CdSe QDs. Inspecting these patterns, no difference could be revealed between PVA pure and that loaded with CdSe quantum dots, which means that no diffraction pattern is obtained for CdSe. Although this may be attributed to the small amount of embedded CdSe, this also indicates that CdSe is homogeneously distributed throughout the PVA. If CdSe was clustered, a diffraction pattern would be obtained even if the amount was small. Nevertheless, there is a small shift for the main peak ($\approx 20^\circ$) towards the smaller angle upon increasing the CdSe concentration, which means that the addition of small percentage of CdSe materials to the PVA modifies the textures of PVA. TEM images of CdSe QDs were used to determine the size and the shape of CdSe QDs. The as-prepared CdSe QD sample made with Cd/Se ratio of 2.2 is shown in Fig. 2a. As seen, the QDs synthesized in this study consisted of basically round particles; most of these particles are of size 2–3 nm. The selected area electron diffraction (SAED) pattern of the QDs is shown in Fig. 2b. Three concentric rings are observed, giving interplanar distances of 0.332, 0.203, and 0.171 nm. Note that, in XRD pattern, there are three diffraction peaks at 27.3° , 45.8° , and 49.2° for the CdSe QDs, and the results of the QDs are in good agreement with those of the XRD pattern. Another interesting point is that the two concentric rings in Fig. 2b are visibly broadened and diffused, a sign of interplanar distance distribution of the QDs. Thus, the rather flat humps in

XRD pattern, Fig. 1a, are related probably not only to the particle size but also to the interplanar distance distribution of the QDs.

Optical characterization

The optical properties of CdSe@PVA composite can be significantly tailored by controlling the size of CdSe particles and the degree of dispersion of CdSe QDs within PVA matrix [14]. The optical properties of CdSe QDs are unique because of its quantum confinement effect leading to increased energy gap between the highest occupied molecular orbitals (HOMO) and lowest unoccupied molecular orbitals (LUMO) [15]. Accordingly, the dispersion of QDs in a polymer matrix is an important issue of any hybrid composite. Semiconductor nanomaterials have a tendency to agglomerate, and inadequate dispersion produces nonuniform films and has a significant impact on the optical properties of nanohybrid materials [15].

UV–visible spectral analysis

The UV–visible absorption spectra of pure PVA and CdSe@PVA composites are shown in Fig. 3a, while Fig. 3b represents the corresponding transmission spectra in the wavelength range from 1100 to 190 nm. The so called “graphical method” [16] can be used for direct estimation of the wavelength value corresponding to absorption edge from the intersection of the sharply decreasing region of the UV–vis spectra with the baseline. It was found that the absorption edge of PVA matrix decreases (blueshifted, 234 nm for pure PVA, 210 nm for $x = 0.001$, and 194 nm for 0.005) once decorated with CdSe QDs and upon increasing in the CdSe content. Furthermore, the UV–vis absorption spectra showed blueshift of about 500 nm with respect to band gap energy of bulk CdSe (712 nm) [17], due to size quantization effect in CdSe particles. Since the absorption edge can be considered as an index

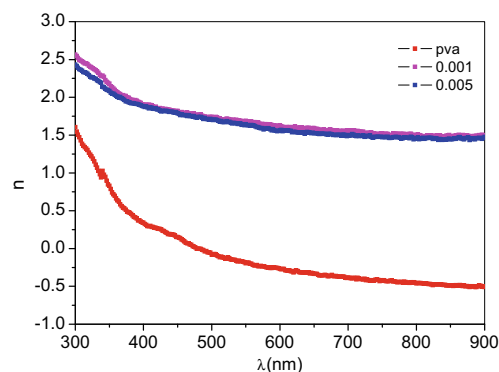


Fig. 5 Variation of refractive index (n) of PVA and CdSe@PVA composites with wavelength

for the particle size [17], the lesser the size, the wider the band gap and absorbs at shorter wavelength. Therefore, the absorption of PVA@CdSe composite system being in the shortest wavelength range of UV region confirms the formation of a quantum composite, for which at least one of its constituent phases (CdSe) is in quantum dot scale that verifies the quantum confinement effect [18]. Moreover, a blueshift is observed upon the increase of CdSe concentration, a result indicating the reduction of particle size with the CdSe content. Other researchers noted the reduction in the particle size upon the increase in the capping agent (CdSe) ratio [19]. The shoulder present in the spectra could be assigned to the optical transition of the first excitonic state [20]. On the other hand, determining the optical band gap has been accepted as a more accurate method for obtaining the wavelength value due to the inherent variation on acquiring the best intersection point from the absorbance spectra [15].

The fundamental absorption corresponding to the transition from the valence band to the conduction band can be used to calculate the band gap of the material. The relation between α and the incident photon energy ($h\nu$) can be written as [12]

$$\alpha h\nu = A(h\nu - E_g)^n, \quad (1)$$

where A is a constant, E_g is the optical band gap of the material, and the exponent n depends on the type of transition. The n may have values 1/2, 2, 3/2, and 3 corresponding to the allowed direct, allowed indirect, forbidden direct, and forbidden indirect transitions, respectively. Figure 4 shows the plot of $(\alpha h\nu)^2$ vs. $h\nu$ for pure PVA as well as for CdSe@PVA composites. The value of optical band gap (E_g) is calculated by extrapolating the straight line portion of $(\alpha h\nu)^2$ vs. $h\nu$ graph

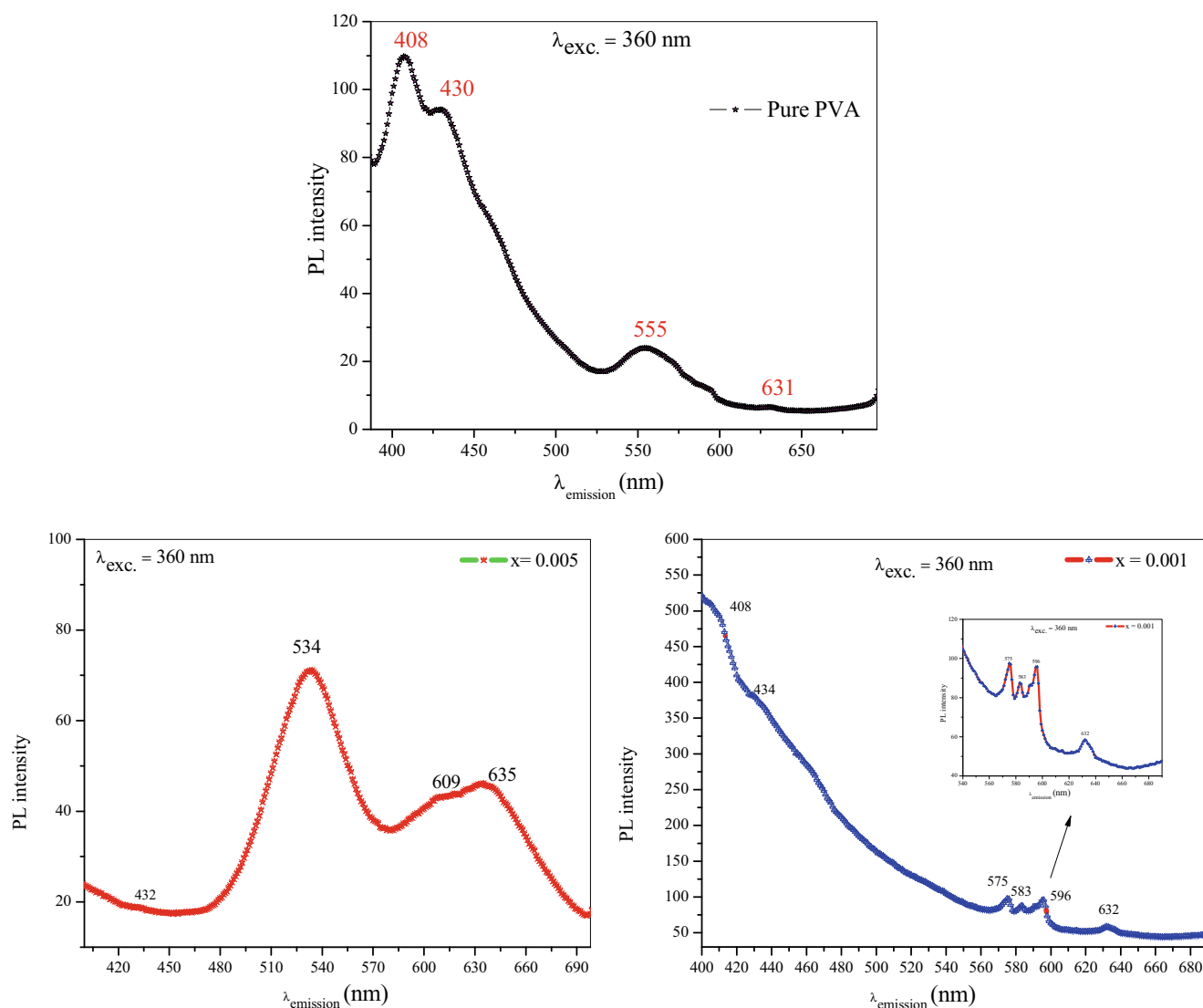


Fig. 6 Room temperature PL spectra of CdSe@PVA composites under 360-nm excitation

to $h\nu$ axis taking $n = 0.5$. The values of the optical band gap for pure PVA and CdSe@PVA composites are 5, 5.27, and 5.34 eV, respectively. These values are in agreement with those estimated from absorption spectra (Fig. 3), where the E_g value (eV) increases with increasing CdSe content ratio. Furthermore, the calculated values of E_g are higher than the value of bulk optical band gap of CdSe [17], a result of quantum confinement. The factor which has a great effect on the size of CdSe is the PVA matrix effect. This blueshift could be attributed to the size reduction effect of a PVA matrix to CdSe QDs. The same observation was reported by S. K. Tripathi et al. [15]. It is observed also that the absorbance of CdSe@PVA composite decreases with the increase of CdSe content ratio, where pure PVA shows the largest absorbance especially at shortest wavelengths. This contradicts with other reported results in the literatures [14] in which the pure PVA shows the lowest absorbance and largest transmittance.

Refractive index is one of the fundamental properties for an optical material because it is closely related to the electronic

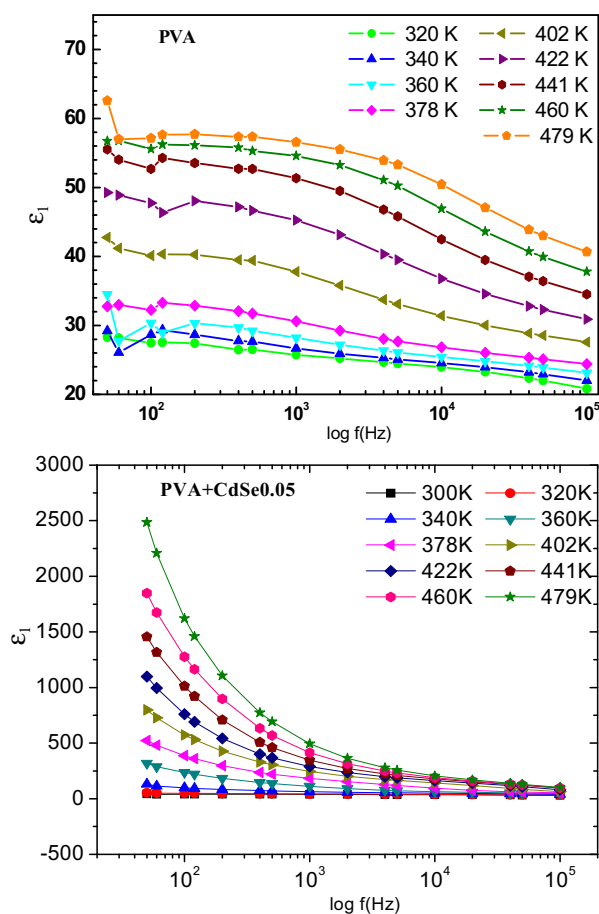


Fig. 7 Variation of dielectric constant (ϵ') for PVA and CdSe@PVA composites as a function of frequency at different temperatures

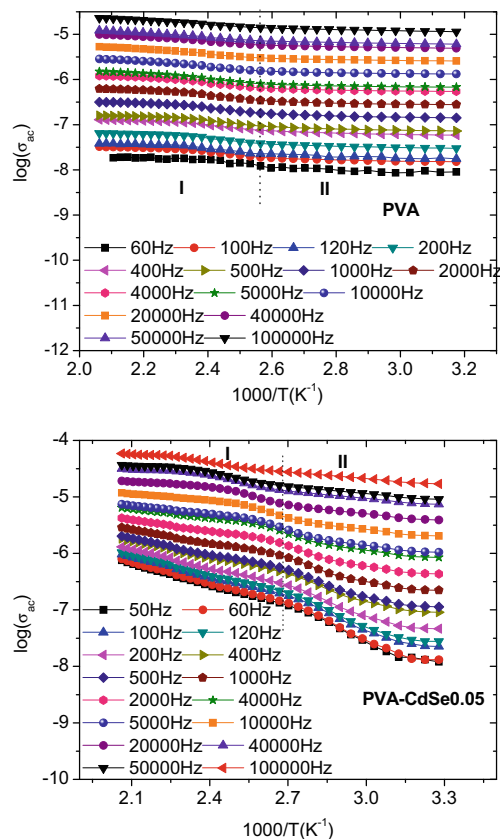


Fig. 8 Variation of $\log(\sigma_{ac})$ with $1000/T$ for PVA and CdSe@PVA composites

polarization of ions and the local field inside materials [10]. One of the methods for calculating the refractive index is by using the extinction coefficient (k) and the reflectance (R) of films [21]:

$$n = \frac{1 + R}{1 - R} + \sqrt{\frac{4R}{(1 - R)^2} - k^2}, \tag{2}$$

where n is the real part of the complex refractive index.

R has been calculated from the absorbance and transmission spectra as

$$R = 1 - \sqrt{T * EXP(A)} \tag{3}$$

and the extinction coefficient (k) can be determined from

$$k = \frac{\lambda\alpha}{4\pi} \tag{4}$$

The spectral distribution of n vs. wavelength λ is shown in Fig. 5. The decrease in the value of n with λ is due to the significant normal dispersion behavior of the composite films. It is noted from Fig. 5 that the refractive index increases with increasing CdSe content ratio. This is attributed to the decrease in the absorbance and subsequent increase in the transmittance with increased CdSe content.

Table 1 The values of the activation energies (E_a) for PVA and CdSe@PVA quantum composites at 1 and 100 kHz

	E_a (eV)			
	1 kHz		100 kHz	
	Region I	Region II	Region I	Region II
PVA	0.68	0.51	0.44	0.13
PVA-CdSe0.05	0.53	0.47	0.32	0.11

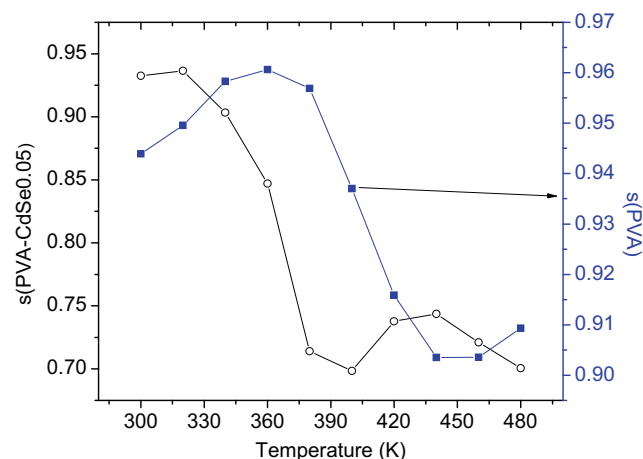
Photoluminescence spectral analysis

The photoemissions from semiconductor nanosystems have different sources like band edge luminescence, non-intentional defect-related luminescence, and luminescence due to doping [22]. The room temperature or relatively low-temperature synthesis methods produce photoluminescence arising from defect levels within the band gap [14]. These defects are usually related to the surface states. In spite of the use of surfactants, these invariably exist in the nanoparticles. It is possible to produce the dopant levels in the band gap and the photoluminescence occur through these levels. Under certain circumstances, photoluminescence due to surfactants or matrix material can be strong enough to dominate the overall luminescence from the particles. Herein, in this work, room temperature photoluminescence was monitored for solid thin film samples of PVA@CdSe composites, Fig. 6. The PL spectra were collected under excitation wavelength of 360 nm of UV light. It is reported in the literature that PVA is a not luminescent material [18], but in the present work, PVA shows luminescent or photoemission peaks under UV absorption or excitation. PVA shows photoemissions at 408, 430, 551, and 631 nm corresponding to violet (408 and 430 nm), green (555 nm), and red (631 nm), respectively. The composite with CdSe QD content ratio of 0.001 shows multicolor emission peaks at 575 and 583 nm (yellow) and 596 nm (orange) and red color emission at 632 nm, while the composite at 0.005 CdSe content emits green color at 534 nm, orange color at 609 nm, and red one at 635 nm. Accordingly, it is clear that the photoemission bands can be controlled with the CdSe wt% and tuned with particle size. Therefore, CdSe QDs can have photoemission peaks anywhere in the visible spectrum, so it is currently being used as multi-color fluorescent markers in biological system. This result is in agreement with others [23] and can be attributed to the quantum confinement of CdSe semiconductor filler within PVA matrix. The CdSe semiconductor material has a large exciton Bohr diameter 12.2 nm, and

therefore its QD form offers the possibility of studying quantum confinement effects in higher cluster size regimes [20]. It is worth to note that there is a blue Stoke's shift in all obtained photoemissions with respect to excitation wavelength, while the broadening of the peak indicates large size distribution at 0.005 composite. The appearance of such broad peak is also reported by M. Sharma et al. [14] for chemically synthesized CdSe doped in PVA polymeric matrix. The larger value of Stoke's shifts for semiconductor nanoparticles dispersed in polymeric media has been reported also by [24, 25]. As reported in the literatures [26, 27], there are two types of photoemission, an excitonic and a trapped emission. The trapped emission is broad and it may be due to the formation of deep or shallow traps. An excitonic emission is normally sharp. In our case, the observed peak at 534 nm is an excitonic emission. The red emission is assigned to the presence of defect-containing materials. The trap states are due to the surface of nanoparticles, which acts as an electron hole acceptor and recombines radiatively.

Dielectric properties

Figure 7 represents the temperature dependence of the dielectric constant (ϵ') of PVA and CdSe@PVA composite films at various frequencies. Remarkably, the dielectric constant (ϵ') decreases systemically upon the increase of the applied frequency. At low temperatures (and a given fixed frequency), the electric dipoles absorb a small amount of the thermal energy that is sufficient only for the dipoles to rotate gently with small angles. At high temperatures, the viscosity of the CdSe/PVA composite decreases; therefore, absorbed thermal energy will be sufficient to orient/rotate the

**Fig. 9** Temperature dependence of exponent s for PVA and CdSe@PVA composites

dipoles along the electric field direction causing a subsequent increase in the polarization [28–30]. It can be seen also from these figures that ε' value increases with the increase in the temperature. From the plotted data also, ε' decreases when the applied frequency increases because the number of dipoles that contribute to the polarization process decreases. The general behavior of ε' is typical of polar dielectrics in which the orientation of dipoles is enabled with the rising temperatures which were rigidly fixed at a lower temperature, therefore responding to electric field. Thus, due to the increase in polarization, the dielectric constant is also increased [31]. In addition, the value of ε' has been enhanced by the addition of CdSe to PVA polymer due to the presence of all the different types of polarizations (interface, dipole, ionic, atomic, electronic, etc.), and the dielectric constant increases with rise in temperature for all the frequencies in addition of the small size of CdSe particles. On the other hand, there are many factors affecting the value of ε' , among them are the electrode polarization, the own dielectric properties of each phase in the composite, and the effect of interfacial region between the two phases within the composite system. Figure 8 shows the variation of the observed a.c. conductivity, $\log(\sigma_{ac})$, with the reciprocal of temperature, $(1000/T)$, for PVA and CdSe@PVA composite films. Noticeably, the a.c. conductivity of each sample increases with increasing the applied frequency. Such temperature dependence of σ_{ac} can be explained as follows: the mobility of polymer chains increases and the fraction of free volume inside the polymer matrix increases with increasing temperature, where the thermal energy facilitates the segmental motion of the polymer blend chains and leads to an enhancement in σ_{ac} at elevated temperatures. Also Fig. 8 shows that the conductivity has been enhanced with the presence of CdSe in PVA matrix. This indicates that the CdSe@PVA composites have been thermally activated, which can be explained on the way that the ions “jump” into the neighboring vacant sites and cause an increase in the conductivity. This behavior can be described by using Arrhenius relation [32]:

$$\sigma_{ac} = \sigma_0 \exp(-E_a/KT),$$

where σ_0 is a pre-exponential factor and k is Boltzmann's constant.

Inspecting Fig. 8, the overall temperature-dependent conductivity curves can be separated into two distinct regions (I and II) which follow the Arrhenius relationship. This may be attributed to the available thermal activation of the polymer chains and also due to the phase transition of the polymer system from semicrystalline to amorphous. The estimated

values of E_a (at 10 and 100 kHz) are listed in Table 1. In general, E_a decreases with the presence of CdSe in the polymer composite. The reduction of E_a and increase in conductivity reflect that CdSe@PVA composite film is more conductive than pure PVA.

For disordered materials, the variation of the electrical a.c. conductivity with the applied frequency is represented by the following expression [33]:

$$\sigma_{total} = \sigma_0 + A(T) \omega^s,$$

where $A(T)$ is a parameter depending on the temperature, ω is the angular frequency ($\omega = 2\pi f$) and s is the exponent power which is in the range from 0 to 1. For $s = 0$, the electrical conduction becomes d.c. one, while for $s > 0$, the conduction is an a.c. conduction [34, 35]. Different models were developed for the frequency and temperature dependence of σ_{ac} and s . Generally, the exponent s varies with temperature and its behavior can help us to explain the hopping conduction mechanism in the investigated composite. It is reported that the small polarons (SP) conduction mechanism is the expected mechanism when the exponent s increases with increasing temperature. On the other hand, the correlated barrier hopping (CBH) is considered a dominant conduction mechanism when s decreases upon increasing temperature. Overlapping large polarons (OLP) could be the dominated conduction mechanism if there is a linear decrease of the exponent s with the temperature such that when the s reaches to a minimum value, it starts to increase again with temperature [36]. The conductivity exponent (s) value can be obtained from the slope of the $\log \sigma$ vs. $\log \omega$ plot. The variation of the obtained values for s with temperature is shown in Fig. 9. It is observed for CdSe@PVA, and nearly for PVA, that by increasing the temperature, s decreases at first then increases a little; this means that both samples follow the OLP model. There is a shift in the minimum value of s for CdSe@PVA composite relative to pure PVA.

Conclusion

CdSe QDs were prepared as a single-phase cubic zinc blende structure with uniform size and good crystallization and then applied successfully to fabricate CdSe@PVA nanocomposite films. The UV–vis absorption spectra showed blue Stoke's shifts of about 500 nm with respect to band gap energy of bulk CdSe (712 nm) due to size quantization effect in CdSe. It was found that the refractive index (n) of PVA increased with introducing CdSe QDs. Photoemission bands could be controlled by CdSe wt% which in turn tuned with the particle size. Multicolor emission bands were observed at both UV and visible range in photoluminescence (PL) spectrum of CdSe@PVA composites. The photoemission in the visible

spectrum region recommends CdSe@PVA nanocomposite for multicolor fluorescent marker fabrication. The dielectric properties and electric conductivity of PVA were enhanced by CdSe QD inset in PVA matrix. The conduction mechanism in PVA@CdSe nanocomposites could be interpreted by the OLP model.

References

- Borkovska L, Korsunska N, Stara T, Gudymenko O, Ye V, Stroyuk O, Raevska O, Kryshchak T (2013) Enhancement of the photoluminescence in CdSe quantum dot–polyvinyl alcohol composite by light irradiation. *Appl Surface Sci* 281:118–122
- Tomczak N, Janczewski D, Han M, Vancso GJ (2009) Designer polymer–quantum dot architectures. *Prog Polym Sci* 34:393–430
- DeMerlis CC, Schoneker DR (2003) Review of the oral toxicity of polyvinyl alcohol (PVA). *Food Chem Toxicol* 41:319–326
- Pritchard JG (1970) *Poly (vinyl alcohol); basic properties and uses*. Gordon and Breach, London, New York
- Trindale T, Brien PO, Pickett NL (2001) Nanocrystalline semiconductors: synthesis, properties, and perspectives. *Chem Mater* 13:3843–3858
- Azizian-Kalandaragh Y, Khodayari A (2010) Ultrasound-assisted preparation of CdSe nanocrystals in the presence of polyvinyl alcohol as a capping agent. *Mater Sci Semicond Process* 13:225–230
- Krishnakumar V, Shanmugam G, Nagalakshmi R (2012) Large third-order optical nonlinearity of Mg-doped PbS/PVA freestanding nanocomposite films. *J Phys D Appl Phys* 45:165102
- Sharma M, Sharma AB, Mishra N, Pandey RK (2011) Investigation of size dependent structural and optical properties of thin films of CdSe quantum dots. *Mater Res Bull* 46:453–459
- Sholin V, Breeze AJ, Anderson IE, Sahoo Y, Reddy D, Carter SA (2008) All-inorganic CdSe/PbSe nanoparticle solar cells. *Energy Mater Sol Cells* 92:1706–1711
- Rodriguez-Carvajal (1993) Recent advances in magnetic structure determination by neutron powder diffraction. *J Physica B (Amsterdam)* 192:55
- L. Lutterotti, Maud 2.33, <http://www.ing.unitn.it/~maud/>
- Heiba ZK, Mohamed MB, Imam NG (2015) Biphasic quantum dots of cubic and hexagonal Mn doped CdS; necessity of Rietveld analysis. *J Alloys Compd* 618:280–286
- Heiba ZK, Imam NG, Mohamed MB (2015) Coexistence of cubic and hexagonal phases of Cd doped ZnS at different annealing temperatures. *Mater Sci Semicond Process* 34:39–44
- Mamta S, Tripathi SK (2013) Photoluminescence study of CdSe nanorods embedded in a PVA matrix. *J Lumin* 135:327–334
- Tripathi SK, Sharma M (2013) Synthesis and optical study of green light emitting polymer coated CdSe/ZnSe core/shell nanocrystals. *Mater Res Bull* 48:1837–1844
- Mansur HS, Mansur AAP (2011) CdSe quantum dots stabilized by carboxylic-functionalized PVA: synthesis and UV–vis spectroscopy characterization. *Mater Chem Phys* 125:709–717
- Khanna PK, Singh N, Charan S, Lonka SP, Reddy AS, Patil Y, Viswanath AK (2006) The processing of CdSe/polymer nanocomposites via solution organometallic chemistry. *Mater Chem Phys* 97:288–294
- Seoudi R, Abd El Mongy S, Shabaka AA (2008) Effect of polyvinyl alcohol matrices on the structural and spectroscopic studies of Cd Se nanoparticles. *Physica B* 403:1781–1786
- Costanzo PJ, Patten TE, Seery TAP (2004) Protein–ligand mediated aggregation of nanoparticles: a study of synthesis and assembly mechanism. *Chem Mater* 16:1775–1785
- Ramrakhiani M, Nogriya V (2013) Photo and electro-luminescence of cadmium selenide nanocrystals and nanocomposites. *J Lumin* 133:129–134
- Migahed M, Zidan HM (2006) Influence of UV-irradiation on the structure and optical properties of polycarbonate films. *Curr Appl Phys* 6:91–96
- Imam NG, Mohamed MB (2014) Optical properties of diluted magnetic semiconductor Cu:ZnS quantum dots. *Superlattice Microsc* 73:203–213
- Kortan AR, Hull R, Opila RL, Bawendi MG, Steigerwald ML, Carroll PJ, Brus LE (1990) Nucleation and growth of cadmium selenide on zinc sulfide quantum crystallite seeds, and vice versa, in inverse micelle media. *J Am Chem Soc* 112:1327–1332
- Talpin DV, Nelson JH, Shevchenko EV, Aloni S, Sadtler B, Alivisatos AP (2007) Seeded growth of highly luminescent CdSe/CdS nanoheterostructures with rod and tetrapod morphologies. *Nano Lett* 7:2951–2959
- Cai W, Li Z, Sui J (2008) A facile single-source route to CdS nanorods. *Nanotechnology* 19:465606
- Mostafa NY, Mohamed MB, Imam NG, Alhamyani M, Heiba ZK (2015) Electrical and optical properties of hydrogen titanate nanotube/PANI hybrid nanocomposites. *Colloid Polym Sci*. doi:10.1007/s00396-015-3769-3
- Heiba ZK, Mohamed MB, Imam NG (2015) Structural tuning of CdS nanoparticles with nucleation temperature and its reflection on the optical properties. *J Mol Struct* 1094:91–97. doi:10.1016/j.molstruc.2015.04.003
- Ghanipour M, Dorrani D, Nanomater J (2013) Effect of Ag-nanoparticles doped in polyvinyl alcohol on the structural and optical properties of PVA films. Article ID 897043:10
- Belal A, Amin M, Hassan H, Abd El-Mongy A, Kamal B, Ibrahim K (1994) The role of BaTiO₃ on the dielectric properties of polyvinyl chloride. *Phys Status Solidi A* 144:k53–k57
- Hanafy TA (2008) Dielectric relaxation and alternating-current conductivity of gadolinium-doped poly(vinyl alcohol). *J Appl Polym Sci* 108:2540–2549
- Heiba ZK, Mohamed MB, Ahmed MA, Moussa MAA, Hamdeh HH (2014) Cation distribution and dielectric properties of nanocrystalline gallium substituted nickel ferrite. *J Alloy Compd* 586:773–781
- Austin IG, Mott NF (1969) Polarons in crystalline and non-crystalline materials. *Adv Phys* 18(71):41–102
- Jonscher AKJ (1986) *Dielectric relaxation in solids*. Chelsea Dielectric Press Limited, London
- Farea AMM, Kumar S, Batoo KM, Yousef A, Lee CG, Alimuddin (2008) Structure and electrical properties of Co_{0.5}Cd_xFe_{2.5-x}O₄ ferrites. *J. Alloy Compd* 464:361–369
- Groothues H, Kremer F, Schouten PG, Warman JM (1995) Charge transport and molecular dynamics in columnar stacks of liquid crystalline phthalocyanine derivatives. *Adv Mater* 7:283–286
- Elliott SR (1987) A.c. conduction in amorphous chalcogenide and pnictide semiconductors. *Adv Phys* 36:135–217